Simulation of Gas Micro Flows based on Finite Element and Finite Volume Method

Armin WESTERKAMP [1,*], Jonas BÜNGER [1], Manuel TORRILHON [1]

* Corresponding author: Email: westerkamp@mathcces.rwth-aachen.de
1: Center for Computational Engineering Science,
Department of Mathematics,
RWTH Aachen University, Germany

Abstract The Regularized 13-Moment Equations state a model for describing rarefied gas flows. The equations are based on a moment approximation of the Boltzmann equation and aim at an accurate prediction up to Knudsen numbers of 0.5. This paper is concerned with the numerical treatment of the PDE system, with special focus on slow flows. Finite elements and finite volumes are applied and the results of both approaches are discussed and the pros and cons are outlined.

Keywords: Kinetic Theory, Moment Methods, Rarefied Gas Flow, Micro Flow

1. Introduction

The accurate prediction of rarefied gas flows via numerical simulation remains a challenging task nowadays. Although the branch of computational fluid dynamics (CFD) has undergone a remarkable development, rarefied gas flows have been excluded from this particular success story. While standard CFD relies on the applicability of the Navier-Stokes equations, choosing an appropriate equation set in the rarefied regime is by no means a straight forward task. In situations where the Knudsen number, which is defined as the mean free path divided by a macroscopic length scale, becomes large, the field of non-equilibrium thermodynamics comes into play. This in turn demands for a non-standard treatment. It is widely accepted that kinetic theory in terms of the Boltzmann equation is able to meet those requirements. In comparison to the macroscopic point of view, that is dominant in standard fluid dynamics, kinetic theory comes along with a microscopic perspective on quantities like temperature and heat. This means in particular a shift from measurable quantities to a statistical description of molecules. But solving the Boltzmann equation numerically is almost forbiddingly expensive due to its high dimensionality. In addition to three spatial and one temporal dimension, also three dimensions in phase space are considered. The phase space thereby spans the space of all possible particle velocities. The goal with moments methods lies within the efficient elimination of the particle velocities as independent variable. This is done by projecting the Boltzmann equation onto a subspace of the velocity space. The resulting equation set is not closed, since there appears one unknown more than equations. This demands for closure, which in particular means a relation of the highest moment to the lower order moments is required. Such a closure gathers all physical modeling and mathematical considerations. Yet, there has not been proposed a closure yielding equations superior in stability and accuracy. But among the contenders, the regularized 13-moment equations (R13) have been shown to be a promising option when it comes to moderate Knudsen numbers up to $Kn = 0.5$. These equations have been introduced in [1], and are extensively discussed in the text book [2]. To get a better picture, the R13 equation set can be understood as a non-equilibrium extension to the

Navier-Stokes-Fourier (NSF) system. In contrast to classical gas dynamics, the heat flux and the stress tensor are introduced as additional unknowns. The standard closures of Navier-Stokes and Fourier are replaced by higher order closures that originate in the so-called order of magnitude method, see [2].

The intent of this paper is to put focus on a specific challenge, namely the handling of curved boundaries, that arises in the overall numerical treatment of the full R13 equation set. Besides discussing a small model problem, a more realistic case is presented in the end in order to demonstrate the promising properties of the model.

2. Challenges in Numerical Methods

2.1 Motivation

When it comes to the numerical simulation of rarefied gas flows, the Direct Simulation Monte Carlo (DSMC) method is the biggest competitor. This particle method is the quasi-standard for most rarefied regimes and is described extensively in [3]. But besides its costly application, computing slow flows with DSMC leads to noisy results. In contrast, the field of slow flows is intended to be one of the main application areas for R13. Slow rarefied flows occur for example in micro systems. Since the macroscopic length scale becomes small, larger Knudsen numbers and therefore rarefaction effects may appear. In that sense, the R13 equations can become a valuable contender particularly when considering engineering practice. For instance, such applications are Knudsen pumps or micropropulsion systems for spacecrafts, see [4] and [5].

2.2 Slow Flows

Taking a closer look on slow flows, a linearization of the equation set with respect to the Mach number is expected to give first insight into the capabilities of R13. In addition, it simplifies the numerical discretization, since dealing with non-linearities does not have to be taken into account. The discretization of the full

R13 system is thereby intended to be done in a step-by-step fashion. First a linear steady state PDE set is analyzed. It is obtained by deriving the first order perturbation around an equilibrium state. In the intended field of application, e.g. micro channel flows, the Mach usually is very small and rarely exceeds a value of unity. Therefore, justification for this approach is also obtained from the perspective of application. In addition, the system has been non-dimensionalized. This yields

$$\frac{2}{5}(\nabla \underline{s})_{\text{sym}} + (\nabla \underline{u})_{\text{sym}} + \frac{1}{\text{Kn}}\underline{\underline{\sigma}} = \frac{6}{5}\,\text{Kn}\,\Delta\underline{\underline{\sigma}}, \quad (1a)$$

$$\nabla \cdot \underline{\underline{\sigma}} + \frac{5}{2}\nabla\theta + \frac{2}{3\text{Kn}}\underline{s} = \frac{6}{5}\,\text{Kn}\,\Delta\underline{s}, \quad (1b)$$

$$\nabla p + \nabla \cdot \underline{\underline{\sigma}} = 0, \quad (1c)$$

$$\nabla \cdot \underline{u} = 0, \quad (1d)$$

$$\nabla \cdot \underline{s} = 0, \quad (1e)$$

where the Knudsen number remains the only parameter. Equations (1c), (1d) and (1e) state the conservation of momentum, mass and energy. Equations (1a) and (1b) are additional constitutive relations, which are closures that go beyond the standard relations of Navier-Stokes and Fourier. Looking at the PDEs from the perspective of standard CFD, we can identify several similarities. To clarify this idea, we first need to understand that in the case of slow flows the NSF system becomes the Stokes equation, with velocity and pressure as unknowns. The temperature distribution is then given by Laplace's equation. Coming back to the linearized R13 system, we first neglect the Laplacian of the heat flux and the stress tensor. Furthermore, by neglecting the coupling terms $(\nabla \underline{s})_{\text{sym}}$ and $\nabla \cdot \underline{\underline{\sigma}}$ in equations (1a) and (1b), we exactly obtain the Stokes equation for velocity and pressure and Laplace's equation for the temperature distribution. Even in the non-linear case, the hydrodynamic counterpart, given by the full Navier-Stokes- Fourier system, is contained.

For this PDE set to valuable, the topic of boundary conditions has to be covered as well. R13 comes along with a full set of solid wall boundary conditions. These have been derived by utilizing Maxwell's accommodation model and

were first stated in [6]. A simplified version of these will be discussed at a later point. For the linearized case combined with the above mentioned solid wall conditions, analytic solutions for flows around a cylinder and a sphere have been derived. Although these cases are quite academic, they are not trivial and already reveal some of the properties of R13. These are for example Knudsen layers, that connect the bulk flow with the conditions at the wall. The occurrence of Knudsen layers has been confirmed by experiments, but cannot be predicted by the NSF model.

The following sections present an entry into to the numerical treatment of the full non-linear R13 system. The long-term objective thereby is to further explore the predictive qualities concerning rarefied gas flows.

2.3 Starting Point

For discussing a first numerical approach, we use equations (1a) - (1e), but this time neglect all coefficients to have a better view on the mathematical structure. We restate the bulk equations

$$(\nabla \underline{s})_{\text{sym}} + (\nabla \underline{u})_{\text{sym}} + \underline{\underline{\sigma}} = \Delta \underline{\underline{\sigma}}, \quad (2a)$$

$$\nabla \cdot \underline{\underline{\sigma}} + \nabla \theta + \underline{s} = \Delta \underline{s}, \quad (2b)$$

$$\nabla p + \nabla \cdot \underline{\underline{\sigma}} = 0, \quad (2c)$$

$$\nabla \cdot \underline{u} = 0, \quad (2d)$$

$$\nabla \cdot \underline{s} = 0, \quad (2e)$$

augmented with a color-coding. The green PDE set describes the transport of heat, where in comparison to the simple Laplacian for the temperature, it is of a Stokes-like structure. The blue set of equations describes the transport of momentum. In comparison to the heat transport equation it has a two-fold saddle point structure. In the standard Stokes equation the pressure acts as a Lagrange multiplier to enforce the continuity constraint, while in the R13 momentum transport the velocity appears as a second Lagrange multiplier. This poses an additional challenge for numerical schemes.

Again, one of the most important contributions of the R13 theory is a full set of solid wall
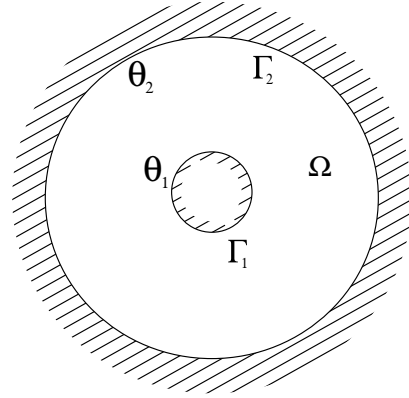

Figure 1: Radial symmetric domain

boundary conditions. In a strongly reduced version, these read

$$u_n = 0, \quad (3a)$$

$$\sigma_{nt_i} = \alpha_1 u_{t_i} + \beta_1 s_{t_i}, \quad (3b)$$

$$-\partial_n \sigma_{nn} = \gamma_1 \sigma_{nn} - \delta_1 (\theta - \theta_w), \quad (3c)$$

$$s_n = \alpha_2 (\theta - \theta_w) + \beta_2 \sigma_{nn}, \quad (3d)$$

$$-\partial_n s_{t_i} = \gamma_2 s_{t_i} - \delta_2 u_{t_i}, \quad (3e)$$

where n and t denote the normal and tangential direction and i distinguishes between the two independent directions in the tangential plane in 3D. Furthermore, all coefficients are strictly positive. The signs originate in kinetic theory but are also crucial for the stability of the numerical scheme.

2.4 Heat Flux problem

Before introducing the actual discretization, we simplify the set of equations even further. We first isolate the heat transport system with the corresponding boundary conditions. We therefore consider the problem

$$\nabla \theta + \underline{s} = \Delta \underline{s}, \quad (4a)$$

$$\text{div } \underline{s} = 0, \quad (4b)$$

with boundary conditions

$$s_n = \alpha_2 (\theta - \theta_w), \quad (5a)$$

$$-\partial_n s_t = \gamma_2 s_t, \quad (5b)$$

on the domain Ω shown in Figure 1. θ_1 and θ_2 are prescribed wall temperatures θ_w at the

boundaries Γ_1 and Γ_2. We choose the ratio $\theta_1/\theta_2 = 4$ and the parameters α_2, γ_2 are set to unity. This concrete problem has been inspired by the Pirani gauge, which measures pressures in vacuum systems via heat loss between two coaxial cylinders.

While discretizing Stokes' equation has been extensively discussed in the literature, e.g. [7], implementing the stated boundary conditions is by no means straight forward. In particular, the coupling boundary condition for the normal component of the heat flux states a major obstacle. The above stated problem serves as a benchmark for the numerical method. It includes a non-trivial geometry and a non-standard boundary conditions, which serve as a prototype for the full set of solid wall conditions.

3. Finite Elements

Since the presented linear system is of elliptic type, the finite element method is a natural choice. But before we turn to the concrete weak formulation, we recall the bulk system being of a saddle-point structure, which means satisfying the so-called inf-sup condition is necessary. In short, this means the choice of discrete subspaces for the vector and scalar quantity is very restricted. A popular pair of finite elements is the Taylor-Hood element, where a standard nodal Lagrange discretization is used and the vector valued quantity is of one order higher than the scalar one. The weak form is given by

Find $(\underline{s}, \theta) \in \{V \times Q\}$, **such that**

$$\int_\Omega \langle \nabla \underline{s}, \nabla \underline{r} \rangle \, dx - \int_{\partial\Omega} \langle \nabla \underline{s} \cdot \underline{n}, \underline{r} \rangle \, dl + \int_\Omega \underline{s} \cdot \underline{r} \, dx$$
$$- \int_\Omega \theta \operatorname{div} \underline{r} \, dx + \int_{\partial\Omega} \theta \langle \underline{r}, \underline{n} \rangle \, dl = 0,$$

$$- \int_\Omega \operatorname{div} \underline{s} \, \kappa \, dx = 0,$$

for all $(\underline{r}, \kappa) \in \{V \times Q\}$

where r and κ state the corresponding test functions for heat flux and temperature respectively. Splitting the boundary integral according to

normal and tangential direction, we obtain

$$\langle \nabla \underline{s} \cdot \underline{n}, \underline{r} \rangle = \partial_n s_n \, r_n + \partial_n s_t \, r_t,$$

which is only possible in 2D. We directly recognize that condition 5b can be inserted in natural fashion, while it is not obvious how to deal with condition 5a. Indeed, it is not expected to find weak formulation that is able to implement both conditions naturally. Numerous formulations have been tested, but shall not be discussed in this context. The interested reader is referred to [8]. A very flexible method to deal with a broad class boundary conditions is given by the penalty method. This method was originally presented to impose Dirichlet conditions in a weak sense by setting up an auxiliary Robin formulation. Given the above stated condition for the normal component of the heat flux, the corresponding penalty formulation reads

$$-\partial_n s_n = \frac{1}{\epsilon}(s_n - \alpha(\theta - \theta_w)), \qquad (6)$$

where $\frac{1}{\epsilon}$ is the penalty parameter. ϵ is typically chosen to be small, so that $\frac{1}{\epsilon}$ is a large factor. This means a scale separation is induced, such that the boundary condition is enforced on a larger scale. The major drawback of this method is the increasing condition number of the system matrix, since this method produces large numbers on some of the diagonal entries. This has to be specifically addressed when designing preconditioners.

4. Finite Volumes and OpenFOAM

4.1 Motivation

In order to understand the motivation of looking at a different method of discretization, the overall goal has to be clarified. At the end of the whole project, an R13 solver has to be implemented that is suitable for real-life applications as they appear in engineering practice. For this task to be a matter of months and not years, libraries providing efficient vector and matrix structures, linear equation solvers, etc. have to be considered. On top of that, toolboxes that cover the complete process from discretizing differential operators to setting up a

system of linear equations and solving it, are taken into account. In the case of CFD-type applications, the software package OpenFOAM is a natural choice. It is todays leading open source CFD toolbox. Developing own applications in OpenFOAM is comfortable because the wide range of provided CFD functionalities and utilities can be used in high-level programming and intuitive interfaces. A clean and object oriented structure allows to become acquainted with the code quickly such that even more complex adaptions can be implemented elegantly. Another strong argument for using OpenFOAM is its ability to parallelize computations without much effort which allows to extend simulations to larger and more complex problems. The toolbox is based on the finite volume method. In the next subsections, the procedure to solve the heat flux problem with extended boundary conditions is outlined. This is then followed by the results that were obtained using OpenFOAM.

4.2 Artificial Compressibility

Among the different established methods for treating incompressible flows with the finite volume method, the artificial compressibility approach has been chosen. The basic concept of the artificial compressibility method for solving incompressible flows is adding a weighted time derivative of the pressure to the continuity equation. Thus creating an auxiliary problem containing an equation for the pressure so that both subsystems can be solved independently. Transferring this concept to the system for transport of heat yields the following system of equations

$$\partial_t \underline{s} + \underline{\nabla}\theta + \underline{s} = \triangle \underline{s} \tag{7a}$$

$$\frac{1}{\beta}\partial_t \theta + \underline{\nabla} \cdot \underline{s} = 0 \tag{7b}$$

β is called artificial compressibility parameter in the context of incompressible flow. The idea is to solve for steady state of the auxiliary problem through time-stepping. In case of steady state the time derivatives vanish and the auxiliary system becomes the steady transport of heat.

Other than for incompressible flows the introduced time derivative of the temperature appears in the unsteady case and is besides the weighting through β not artificial. The value of β influences the efficiency of the method significantly. A large value for β enforces the incompressibility but also makes the equations numerically stiff. Typical values for β used in methods based on artificial compressibility are in between 0.1 and 10, see [9]. Given that the introduced time-derivative is not truly artificial it seems naturally to set β to one.

As every equation in system 7 contains a time derivative a wide range of methods for solving the system is available. A simple and easy to implement approach of solving for steady state is to sequentially update the heat flux and temperature field with the current value for the other. The method used by the authors is illustrated in algorithm 1, where the index h represents discrete finite volume functions and operators.

> initialize $\underline{s}_h^0$, θ_h^0;
> $n = 0$;
> **while** $n \leq n_{end}$ **do**
>> // update s_h
>> set $\underline{s}_h^{n+1}$ at boundaries;
>> $(\Delta t^{-1} + 1 - \Delta_h)\underline{s}_h^{n+1} = \Delta t^{-1}\underline{s}_h^n - \underline{\nabla}_h\theta_h^n$;
>> // update θ_h
>> set θ_h^{n+1} at boundaries;
>> $\theta_h^{n+1} = \theta_h^n - \Delta t\beta\underline{\nabla}_h \cdot \underline{s}_h^{n+1}$;
>> $n = n + 1$;
>
> **end**

Algorithm 1: FV-Solver for transport of heat

4.3 Boundary Conditions

The boundary conditions for the simplified linear transport of heat are

$$s_n = \alpha_2(\theta - \theta_w) \tag{8a}$$

$$-\partial_n s_{t_i} = \gamma_2 s_{t_i} \quad . \tag{8b}$$

Obviously no explicit BC for the gas temperature θ at the wall is stated. The temperature at the boundary is influenced indirectly by the wall

temperature θ_w through the heat flux normal to the boundary.

Implementing the heat flux $s_{h,b}$ at the boundary meets two challenges. Approximating the gas temperature θ in equation 8a and discretizing the directional derivative $\partial_n s_{t_i}$ in equation 8b. The former can be achieved through extrapolation of the internal temperature field onto the boundary patches

$$\theta \approx \theta_{h,extr.} \; . \tag{9}$$

If the mesh at the boundary is such that the line connecting the centers of the boundary patch and cell are parallel to the boundary normal, the derivative can be approximated by a finite difference

$$\partial_n s_{t_i} \approx \frac{s_{h,t_i,p} - s_{h,t_i,b.c.}}{d} \; . \tag{10}$$

Here $s_{h,t_i,p}$ is the heat flux at the boundary patch in direction t_i, $s_{h,t_i,b.c.}$ the projection of the heat flux at the boundary cell onto the direction t_i and d the distance between the cell center and the patch center. Using the values of the previous time-step for the internal field data yields the following explicit update formulas

$$s_{h,n}^{n+1} = \alpha_2(\theta_{h,extr.}^n - \theta_{h,w}^n) \tag{11a}$$

$$s_{h,t_i}^{n+1} = \frac{s_{h,t_i,b.c.}^n}{1 + d\gamma_2} \; . \tag{11b}$$

The heat flux at the boundary then follows from

$$\underline{s}_{h,p}^{n+1} = s_{h,n}^{n+1}\underline{n} + \sum_{i=1}^{2} s_{h,t_i}^{n+1}\underline{t_i} \tag{12}$$

5. Comparison and Discussion

5.1 Results

In the following computations, another problem is outlined which is the proper handling of curved boundaries. When discretizing the Stokes-like heat transport equation with standard $P2 - P1$ Taylor-Hood elements using the penalty method, unphysical oscillations appear near the boundary, as can be seen in Figure 2. It turns out, this problem is likely to occur, when
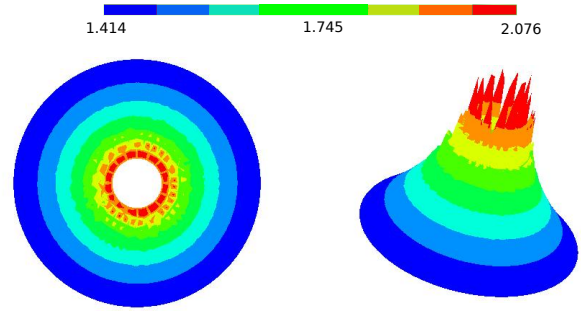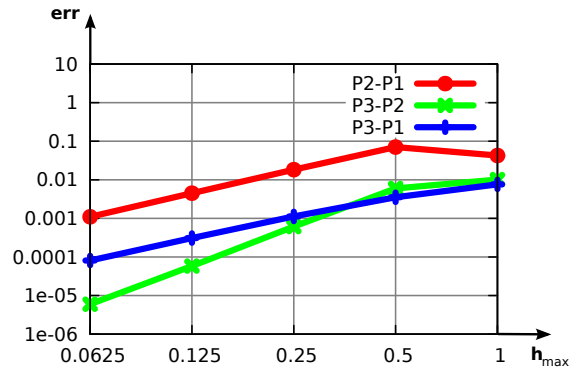

Figure 2: Temperature oscillations (FEM)

Figure 3: Convergence of the scalar quantity for different element pairs

prescribing the normal component of the vector valued quantity on a curved boundary. This even holds for the standard Stokes case. A remedy can be found in augmenting the approximation of the boundary by using isoparametric elements. In this, the standard element transformation is modified for elements that coincide with the boundary. Besides the $P2 - P1$ element, other element pairs, that also fulfill the inf-sup condition, have been tested. This is the $P3 - P2$ and the non-standard $P3 - P1$ element. For all three element pairs the convergence rate of the scalar quantity in the $L2$-norm has been evaluated. The convergence study in the case of isoparametric elements can be seen in Figure 3. It should be remarked that although $L2$-convergence is almost optimal for all element pairs, the $P3 - P1$ outperforms the others regarding the occurrence of the oscillations.

In contrast to FEM, applying the FVM does not result in unphysical modes near the boundary, as shown in Figure 4. This is remarkable, since no additional treatment of the curved boundary has been used. A corresponding convergence
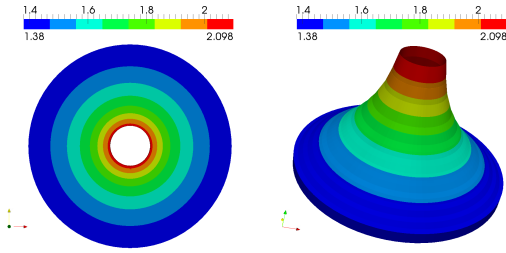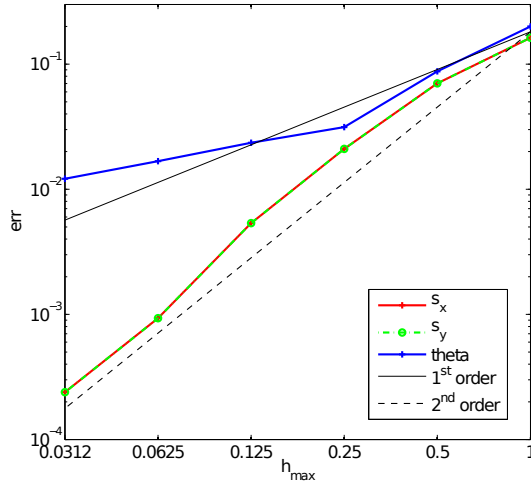
Figure 4: Temperature plot (FVM)

Figure 5: OpenFOAM convergence

analysis is presented in Figure 5. While the heat flux shows optimal order of convergence, the poor result for the temperature surprises. A further investigation of this issue is part of future research.

5.2 Discussion

Both of the outlined methods were able approximate the analytic solution of the two cylinder domain in two dimensions properly. The major difference lies within the solution of the appearing linear equation system. In the case of finite elements, a solution of the coupled steady state system was computed using a direct solver. A stable solution therefore can be computed up to a very high accuracy. This is backed up by the good convergence rates, when applying the isoparametric method. The major drawback lies within the saddle-point structure. For 3D problems, a direct solver is not a good choice anymore due to its vast memory consumption. In such a case, iterative solvers with special pre-

conditioners have to be applied. In contrast to this, the steady state OpenFOAM solution has been computed in a sequential manner by using a time-stepping method. Therefore the equation describing transport of heat has been decoupled from the divergence-free constraint. For the single equations, standard iterative solvers have been applied, which especially allows for the straightforward solution of complex 3D problems. Furthermore, the finite volume approach needs far less degrees of freedom than standard FEM. It is owned to the fact that finite volume only uses cell averages represented by the values at the cell centers. This means only one degree of freedom (DOF) per cell is taken into account. In comparison, finite element methods locally raise the number of DOFs to gain higher order. The disadvantages of the OpenFOAM implementation can be seen in the poor convergence of the temperature. In addition, the stability of such a decoupled approach concerning the convergence of the time-stepping remains questionable for complex problems. At least this can lead to very small time-steps.

5.3 Fully coupled linear system

In order to give an outlook on future achievements, a computation for the completely coupled case ((1a) - (1e)) using the FEM is presented. The details of the discretization for the stress system are skipped, since these are beyond the scope of this paper. The illustration case is a ring shaped channel, where a linear temperature gradient is prescribed along the wall. This triggers a thermal creep flow, like it is present in a Knudsen pump. The case is inspired by [10], where such a geometry was investigated using the DSMC method. The application focuses on making Knudsen pumps more feasible by changing curvature instead of changing the cross section. The computational result is shown in Figure 6, where the arrows indicate the velocity direction and the coloring represents the velocity magnitude. A Knudsen number of 0.5 and a maximum temperature difference of 0.1 has been prescribed. We can clearly see a circulating flow in counter-
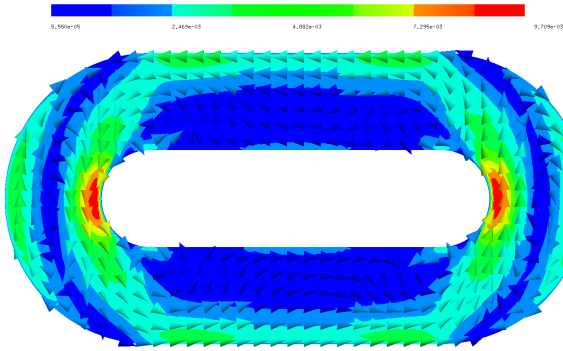
Figure 6: Ring shaped channel with prescribed temperature gradient at the walls

clockwise direction, which is mildly disturbed by recirculations near the curvature. The velocity shown has been scaled with the local speed of sound and ranges from 0 to roughly 0.01. Although simplified model equations and not fine tuned parameters were used, a basic qualitative alignment with the DSMC computations can be observed. This computational illustration therefore gives an impression of what continuum models like R13 can be capable of. Besides fast computations in industrial real-life applications also fields like PDE constrained optimization are made accessible for rarefied flow scenarios. Such methods then greatly add to an engineering toolbox for the design of MEMS devices. Investigations of such problems using OpenFOAM is part of future research.

6. Conclusions and Future Work

The main questions that remain in the presented cases lie within the occurrence of the near boundary oscillations. The OpenFOAM case has to be further investigated to clarify the non-appearance of oscillations. This may be related to the structured radial symmetric quad mesh, where in the FEM case a standard unstructured triangulation was used. Future research will also include a deeper analysis the remaining system for the transport of momentum. In this context, the topic of stabilization will be of particular interest. As a last comment, it should be stated that both methods, finite element and finite volume, will be further pursued.

References

[1] Struchtrup, H. & Torrilhon, M. 2003 Regularization of Grad's 13 moment equations: Derivation and linear analysis. *Phys. Fluids*, **15**(9), 2668–2680.

[2] Struchtrup, H. 2005 *Macroscopic Transport Equations for Rarefied Gas Flows*. Interaction of Mechanics and Mathematics. New York: Springer.

[3] Bird, G. A. 1998 *Molecular Gas Dynamics and the Direct Simulation of Gas Flows*. Oxford University Press, 2nd edn.

[4] McNamara, S. & Gianchandani, Y. B. 2005 On-chip vacuum generated by a micromachined Knudsen pump. *Journal of Microelectromechanical Systems*, **14**(4), 741–746.

[5] Alexeenko, A. A., Fedosov, D. A., Gimelshein, S. F., Levin, D. A. & Collins, R. J. 2006 Transient heat transfer and gas flow in a mems-based thruster. *Journal of Microelectromechanical Systems*, **15**(1), 181–194.

[6] Torrilhon, M. & Struchtrup, H. 2008 Boundary conditions for regularized 13-moment-equations for micro-channel-flows. *Journal of Computational Physics*, **227**(3), 1982–2011.

[7] Braess, D. 2001 *Finite Elements: Theory, Fast Solvers, and Applications in Solid Mechanics*. Cambridge University Press.

[8] Westerkamp, A. 2012 Finite element discretizations for extended gas dynamics. Master's thesis, RWTH Aachen University.

[9] Ferziger, J. H. & Perić, M. 2002 *Computational Methods for Fluid Dynamics*. Springer London.

[10] 2007 *Numerical Simulation of a Knudsen Pump Using the Effect of Curvature of the Channel*. Rarefied Gas Dynamics.